

Correlation between Specimen Size and Fracture Toughness of 1Cr-1/2Ni Cast Steel Used in the Anchorage of a Cable-Stayed Bridge

L. A. Alcaraz-Caracheo¹
J. Terán-Guillén²
F. J. Carrión-Viramontes²
M. Martínez-Madrid²

¹Instituto Politécnico Nacional,
Escuela Superior de Ingeniería Mecánica y Eléctrica,
Sección de Estudios de Posgrado e Investigación.
Av. Instituto Politécnico Nacional s/n, Unidad Profesional
"Adolfo López Mateos", Col. Lindavista,
México, DF, CP 07738.
MÉXICO.

²Instituto Mexicano del Transporte.
km 12 Carretera Querétaro Galindo,
Sanfandila, Querétaro, CP 07670.
MÉXICO.

correo electrónico (email): alexalcaraz@itc.mx,
jorge.teran@imt.mx

Recibido 15-06-2011, aceptado 09-04-2012.

Abstract

The fracture toughness of 1Cr-1/2Ni cast steel, which is used in cable anchorage element, was studied. Subsize specimens were tested following the three-point bending test. Results revealed a quasi-cleavage micromechanism of fracture and a decreasing trend of the apparent fracture toughness as the specimen size decreases. The relation between the size effect on the fracture toughness and the tearing resistance curve shape were established. The value of plane strain fracture toughness has found to be $K_{IC} = 39.4 \pm 6 \text{ MPam}^{1/2}$. In addition, a linear relationship between the normalized apparent toughness K_Q/K_{IC} and the square root of the normalized ligament size have been suggested. It was shown that this relationship is also consistent with experimental data for aluminum and titanium alloys available in the open literature. The methodology employed in this work can be

used in future studies, when available specimen sizes are restricted.

Key words: cast steel, fracture toughness, subsize specimens, size correlation.

Resumen

(Correlación del tamaño de espécimen con la tenacidad a la fractura de un acero colado 1Cr-1/2Ni de un anclaje para un puente atirantado)

La tenacidad a la fractura de un acero colado 1Cr-1/2Ni de un elemento de anclaje de un tirante fue estudiado por el método de flexión en tres puntos usando especímenes pequeños. Los resultados revelan un micro-mecanismo de fractura de cuasi-clivaje y una tendencia de la tenacidad de fractura aparente a disminuir conforme el tamaño del espécimen disminuye. Se establecieron a relación entre el efecto del tamaño del espécimen y la tenacidad a la fractura y, por otra parte, la forma de la curva de resistencia al desgarramiento. El valor de la tenacidad a la fractura en deformación plana fue encontrado de $K_{IC} = 39.4 \pm 6 \text{ MPam}^{1/2}$. Además una relación lineal entre la tenacidad aparente normalizada K_Q/K_{IC} y la raíz cuadrada del tamaño de ligamento normalizado han sido sugeridas. Se mostró que esta relación también es consistente con datos experimentales de aleaciones de aluminio y titanio disponibles en la literatura abierta. La metodología empleada en este trabajo puede ser usada en estudios futuros, cuando los tamaños de especímenes disponibles son limitados.

Palabras clave: acero colado, tenacidad a la fractura, especímenes pequeños, correlación de tamaño.

1. Introduction

Accident failure analysis of structural elements with flaws or cracks requires the knowledge of the material toughness [1,2]. Plane strain fracture toughness (K_{IC}) is commonly measured on precracked specimens following to the ASTM E399 standard testing method, which requires plane strain conditions at the crack tip [3]. However, in many practical situations, the standard testing program cannot be applied. This is the case when the available material is insufficient

to conduct the standardized tests required to obtain K_{IC} . In these cases, K_{IC} has to be estimated with subsize specimens [4-6].

A comprehensive analysis of the plane strain fracture toughness data for metallic alloys, reported in the literature, has shown that K_{IC} varies by more than one or two orders of magnitude, from its lowest to highest value [7]. This scatter, at least partially, can be attributed to the size effect on the fracture toughness [8-12]. In fact, the mechanical properties of structurally inhomogeneous materials, such as cast steels, are strongly affected by the size effect, *i.e.*, they strongly depend on the loaded volume [1]. The size effect is especially pronounced under conditions of stress concentration, when the characteristic size of the dominium of stress concentration is small as compared with the dimensions of specimens used in the evaluation of K_{IC} . Hence, to assess the feasibility of subsize specimens use to estimate K_{IC} , it is necessary to understand how the fracture toughness changes as a function of specimen sizes. Accordingly, the size effect on the fracture toughness has been vividly discussed in the literature for a long time [8-30]. In this context, it was found that the crack roughness can affect the stress distribution at the crack tip vicinity. It leads to a strong scaling dependence of the measured fracture (see Refs. [9,10,14-18] and references therein). On the other hand, some correlations have been suggested to account the specimen thickness for specimens with smooth (straight) notches (see, for example, Refs. [23-30] and references therein). However, these correlation are usually applicable only to obtain the corresponding fitting relations. The absence of fundamental understanding of the size effect in fracture toughness measurements has stimulated further studies to assess the feasibility of the use of subsize specimens to estimate K_{IC} .

This paper was motivated by the need to determine the fracture toughness of the material of a cable anchorage, which is used in a cable-stayed bridge. This was done after three of 112 anchorage have failed during ten years of bridge service. Postaccident analysis has suggested that the structural deficiencies of failed anchorage elements were associated with pores and inclusions. Some concern was raised for the remaining anchorages. Therefore, four of the non-failed anchorages elements were also removed to study their mechanical properties. These properties were used to assess the reliability of the bridge. In this paper, the study of fracture toughness of the 1Cr-1/2Ni cast steel from the non-failed upper anchorage element of one cable has been reported.

The size of anchorages is insufficient to fabricate the standard specimens for the evaluation of the plane strain fracture toughness in according with the ASTM E399 standard testing procedure. Therefore, fracture toughness with subsize

specimens was determined. Furthermore, the tearing resistance curve and fracture micromechanism were analyzed for specimens of different size, while the specimen shape was kept constant. Different size correlation relations were employed to fit our experimental data. A function, which took into account the size effect, was suggested. The viability of this scaling function is discussed using the data of present work in conjunction with the available experimental data in the open for some other material.

2. Experiment details

Four non-failed anchorage elements, removed during the bridge rehabilitation works (see Fig. 1), were used to determine the fracture toughness.

2.1. Material and specimens

The material of cable anchorage is a medium carbon low alloy cast steel with a microstructure of ferrite and pearlite (see Fig. 2a). Typical discontinuities of the casting process, such as sulfide inclusion and pores, can be observed in the optical micrograph shown in Fig. 2b.

The chemical composition of tested steel is given in table 1. Tensile properties at room temperature were obtained in accordance with ASTM standard method E8 [31]. The gage length and thickness of tensile test specimens were of 25 and 6 mm, respectively. The tests were carried out with a stress rate of 1.15 MPa/s on a servo-hydraulic machine. The results of the tensile tests are summarized in table 2 for 0.2% offset yield strength (σ_y), modulus of elasticity (E), ultimate tensile strength (UTS) and percent of elongation (%El).

Regarding the fracture analysis, three-point bending tests were performed with 20 single edge notched specimens (see Fig 3) of four different sizes. The dimensions of the tested specimens are given in table 3. The first two specimens were the largest (1

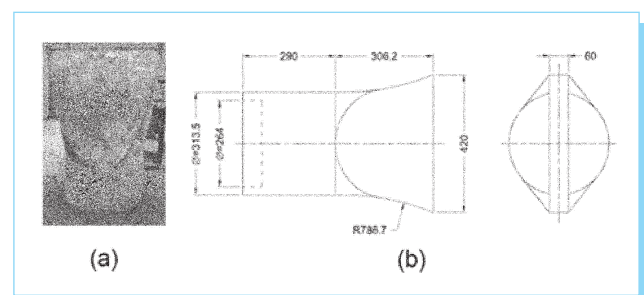


Fig. 1. (a) Steel casting anchorage and (b) its schematic diagram (all dimensions are in mm).

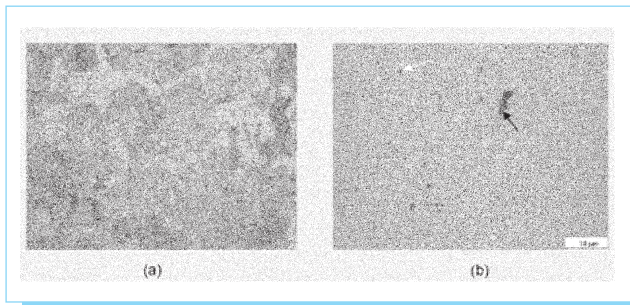


Fig. 2. (a) Microstructure of ferrite and pearlite 3% nital etch. 1000X and (a) micrograph presented manganese sulfide (black arrow) and pore (white arrow). As-polished. 100X.

SE(B)) as shown in Fig. 3a. Once these specimens were tested, smaller specimens were machined from the remaining fractured halves of 1 SE(B) specimens. Specifically, two 0.5 SE(B), three 0.29 SE(B) and four 0.25SE(B) specimens were obtained from each 1 SE(B) specimen, as it is shown in Fig. 3b.

Table 1. Chemical composition of 1Cr-1/2Ni cast steel in wt. %.

C	Mn	Si	S	P	Cr	Mo	Ni	Cu
0.42	0.82	0.80	0.02	0.03	0.03	0.09	0.53	0.34

Table 2. Mechanical properties of 1Cr-1/2Ni cast steel at room temperature.

Modulus of elasticity	Yield strength	Tensile strength	Elongation
199 GPa	323.02 MPa	621.24 MPa	8.38 %

Table 3. Dimensions and number of specimens.

Specimen	Nominal width W (mm)	Nominal thickness B (mm)	Fatigue precrack a_0 (mm)	Number of specimens
1 SE(B)	104	52	56.80	2
0.5 SE(B)	52	26	28.19	4
0.29 SE(B)	30	15	16.19	6
0.25 SE(B)	26	13	14.13	8

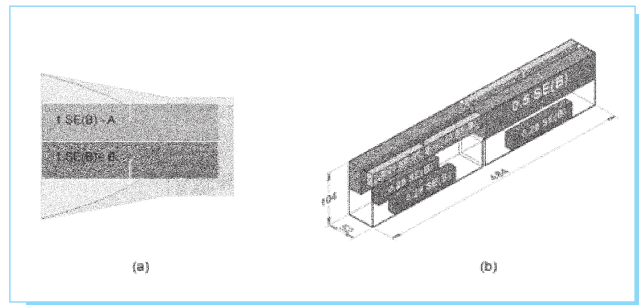


Fig. 3. Test specimen fabrication: (a) orientation of 1 SE(B) specimens within anchorage element and (b) arrangement of 0.5, 0.29 and 0.25 SE(B) specimens within 1 SE(B) specimen.

2.2. Three-point bending tests

Fracture toughness tests were performed at room temperature on a three-point bending fixture following ASTM E399-09 standard test procedure [3]. Tests were carried out on a servo-hydraulic machine. The load was applied with a sinusoidal frequency of 15 Hz and an inversion ratio of $R = 0.1$. The force was measured with a standard load cell of 100 kN and crack opening displacement was recorded using COD gage attached to the integral knife-edges in the specimen (see Fig. 4). Each specimen was fatigue pre-cracked with decreasing ΔK until the a/W ratio was between 0.54 and 0.55. Further, the fracture toughness tests were conducted with an increasing stress intensity factor rate of 0.55 MPam^{1/2}/s until fracture instability at $P = P_{max}$.

Fig. 5 shows typical graphs of load versus the clip gauge displacement. It can be observed that as the specimen size

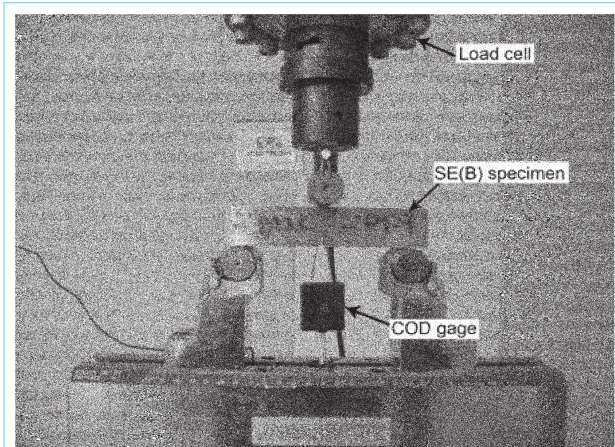


Fig. 4. Setup for three-point bending test.

decreases, the load-displacement plot exhibits a greater deviation from the elastic loading line before reaching the maximum load. Furthermore, in many cases, a jerky behavior of the load accompanied by an audible sound was observed (Fig 5). This "pop-in" behavior can be caused by the inhomogeneity of the material. Accordingly, the apparent toughness K_Q was calculated as follows

$$K_Q = \frac{P_Q S}{BW_0^{3/2}} f(a/W) \quad (1)$$

where the load P_Q is defined in Fig 6, B is the thickness, S is the span, and $f(a/W)$ is the geometric factor defined in [3].

According to ASTM E399 standard [3], K_Q can be taken as the fracture toughness K_{IC} , if the conditions

$$P_{max} / P_Q \leq 1.1 \quad (2)$$

and

$$W - a \geq 2.5 (K_Q / \sigma_y)^2 \quad (3)$$

are accomplished. Otherwise, either a thicker sample should be prepared if possible, or the value of K_Q can be estimated using an appropriate size correlation relation.

3.1. Fractography, tearing resistance curves, and fracture toughness validation

Representative load-displacement curves for each specimen size are shown in Fig. 5. It was observed that the cleavage fracture is preceded by a considerable plasticity and possibly some tearing, while the macroscopic fracture surfaces exhibit typical brittle fracture patterns without shear lips. Accordingly,

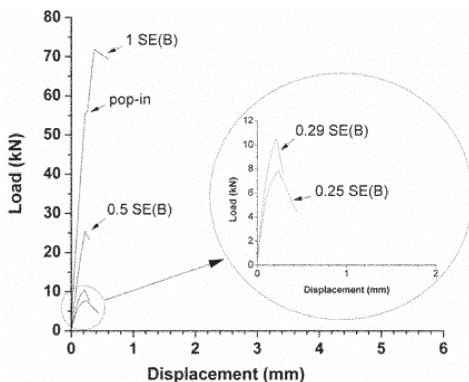


Fig. 5. Load-displacement curves for specimens of different sizes.

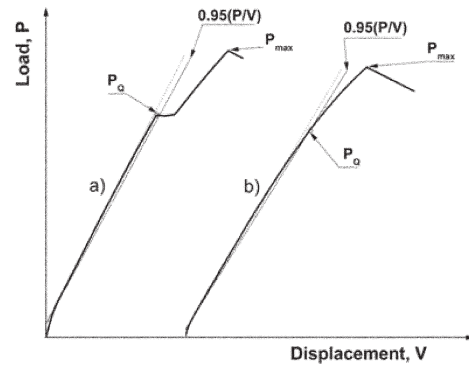


Fig. 6. P_Q established from the force versus crack opening displacement diagram.

extensive fractography was performed over the fractured specimens. Typical fractographs are shown in Fig. 7. In all cases, the fracture surfaces reveal cleavage behavior plus dimples and tear ridges. The size of the dimple region increases, as the specimen size decreases. Besides, most of the crack initiation points were at interfaces such as grain boundaries.

Experimental values of P_{max} and P_Q were obtained with 20 specimens. The results are summarized in table 4. It can be noted that the ratio P_{max}/P_Q tends to decrease as the specimen size increases. However, the condition defined by Eq. (2)

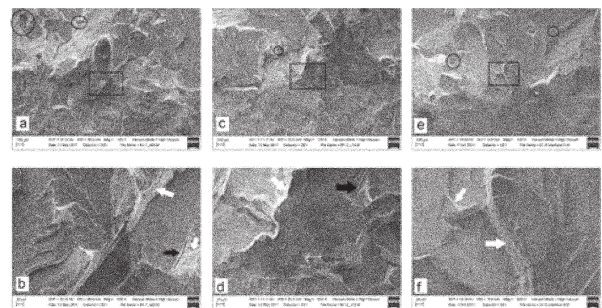


Fig. 7. Fractures SEM micrograph of specimens of different size close to fracture initiation from fatigue precrack. (a) Specimen 1 SE(B). (b) Detail of the rectangle in (a). (c) Specimen 0.5 SE(B). (d) Detail of the rectangle in (c). (e) Specimen 0.25 SE(B). (f) Detail of the rectangle in (e). Note the presence of cavities (circled) in low magnification SEM while secondary cracks (black arrow) and dimples or tear ridges (white arrow) are revealed in high magnification SEM.

was not accomplished (see Fig. 8). In fact, the ratio P_{max}/P_Q is mainly related to the steepness of the tearing resistance curve, which follows the power law scaling

$$K_R = A(\Delta a)^m \quad (4)$$

where A and m are material parameters [2,29]. Wallin [24] has suggested that there is no theoretical justification in the application of the criterion of Eq. (2) as plane-strain measure.

Moreover, it was suggested that only materials with a flat tearing resistance curve ($m < 0.1$) are suitable to meet the criterion $P_{max}/P_Q \leq 1.1$ [2,24,29]. Consequently, when there is brittle behavior and the criterion Eq. (3) is fulfilled, the condition $P_{max}/P_Q \leq 1.1$ can be overlooked if $m > 0.1$.

The effect of ligament size on the apparent toughness is shown Fig. 9. It can be seen that K_Q increases as the specimen size increases. This situation is expected in materials with a

Table 4. Results of fracture toughness test of 1Cr-1/2Ni cast steel.

Specimen	Thickness B (mm)	Width W (mm)	Ligament $W-a$ (mm)	Conditional load P_Q (kN)	Load ratio P_{max}/P_Q	Stress intensity factor K_Q (MPa m ^{1/2})	Estimated K_{IC}^a (MPa m ^{1/2})
1 SE(B)	52.06	104.14	47.16	55.81	1.29	41.80	-
	52.05	104.30	46.81	49.17	1.33	37.01	-
						39.41 ^b 3.39 ^c	
0.5 SE(B)	26.33	52.22	23.70	18.47	1.32	38.10	43.76
	26.64	52.43	24.33	19.62	1.30	38.53	44.52
	26.34	52.21	24.08	16.26	1.56	32.68	37.84
	26.34	52.23	24.37	17.50	1.29	34.55	39.91
						35.97 ^b 2.82 ^c	41.51 ^b 3.17 ^c
0.29 SE(B)	15.05	30.07	13.83	6.30	1.49	29.36	37.50
	14.92	30.02	13.49	6.01	1.65	29.34	37.63
	15.07	30.01	13.76	6.51	1.61	30.44	38.92
	15.09	30.05	14.03	6.05	1.57	28.39	36.18
	15.08	30.04	13.80	6.32	1.48	29.62	37.85
	15.08	30.05	13.54	6.23	1.43	29.94	38.38
						29.52 ^b 0.69 ^c	37.74 ^b 0.93 ^c
0.25 SE(B)	12.81	26.04	11.69	4.78	1.46	29.00	38.03
	13.06	26.09	11.67	4.87	1.61	29.56	38.78
	13.08	26.12	11.56	6.16	1.29	37.54	49.31
	12.81	25.73	11.36	4.54	1.47	28.65	37.74
	12.81	25.67	11.54	4.84	1.18	29.72	39.06
	13.07	26.10	11.72	4.86	1.57	29.03	38.06
	13.05	26.10	11.71	4.75	1.91	28.59	37.49
	12.83	25.78	11.96	4.85	1.45	28.25	36.92
						30.04 ^b 3.07 ^c	39.42 ^b 4.05 ^c

^a estimated K_{IC} calculated using E. 5
^b mean
^c standard deviation

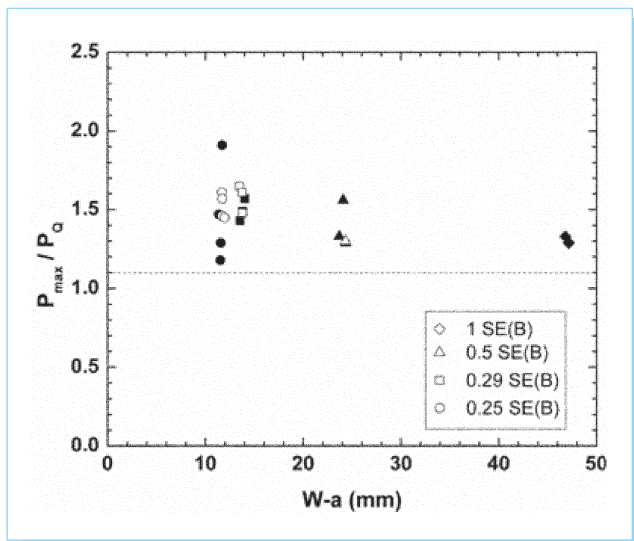


Fig. 8. Ratio P_{max}/P_Q as a function of ligament size $W-a$. Filled symbol represent tests where a pop-in crack extension was recorded.

rising tearing resistance curve [24]. Furthermore, the largest specimens fulfill the criterion defined by Eq. (3), while the requirement defined by Eq. (2) is not accomplished.

Accordingly, to explore the possibility to overlook the criterion $P_{max}/P_Q \leq 1.$, an analysis of the shape of tearing

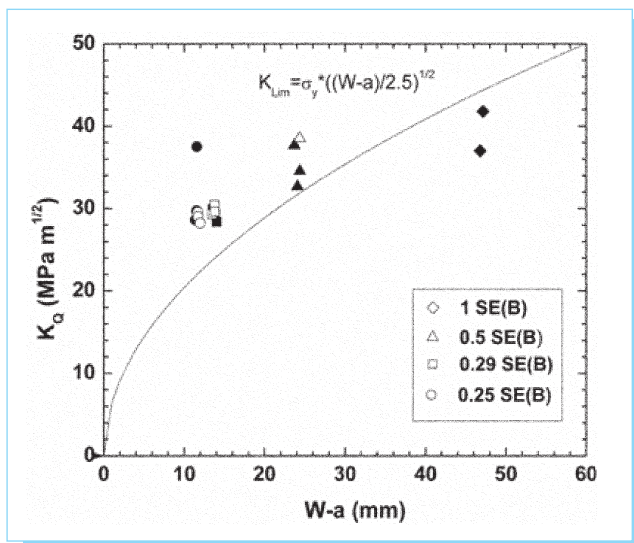


Fig. 9. K_Q as a function of ligament size $W-a$. The curve represents the ASTM E399-09 standard specimen size requirement (3); filled symbols indicate pop-in.

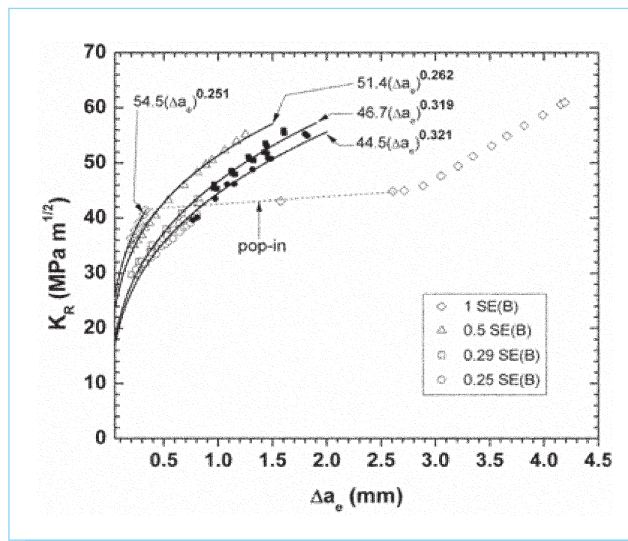


Fig. 10. Tearing resistance curve for all specimen without pop-in, except for 1SE(B) size (filled points indicate $R_v > 1$ according with ASTM E561 [32]).

resistance curve was performed. The tearing resistance curves (see Fig. 10) were constructed with representative data from the toughness tests in accordance with the ASTM E561 standard [32]. Experimental data were fitted with a power law relationship (4). It was found that the scaling exponent decreases as the specimen size increases. Specifically, we found $m = 0.251, 0.262, 0.319,$ and 0.321 for 1 SE(B), 0.5 SE(B), 0.29 SE(B), and 0.25 SE(B) specimens, respectively. These results, together with the trend shown in Fig. 8, confirm the relation between the tearing resistance curve shape and load ratio P_{max}/P_Q . Namely, the smaller values of are associated with the smaller values of P_{max}/P_Q . We also noted that the decrease of the tearing resistance curve steepness for larger specimens is associated with the decrease of the dimple region sizes on the fracture surface (see Fig. 7). Therefore the apparent toughness K_Q of the largest specimens 1 SE(B) can be taken as a valid fracture toughness K_{IC} (see table 4).

Furthermore, a linear correlation between the apparent toughness K_Q and ratio P_{max}/P_Q (see Fig. 11) was found. This estimates an equivalent fracture toughness $K_{1.0}$ by the extrapolation of $K_Q(P_{max}/P_Q)$ to the limit at $P_{max}/P_Q = 1$ [30]. In this way, $K_{1.0} = 45.5 \text{ MPa m}^{1/2}$ was estimated (see Fig. 11). It is almost 9% larger than the closest experimental value of $K_Q = 41.8 \text{ MPa m}^{1/2}$ and 13.4% larger than the mean value $K_Q = 39.4 \text{ MPa m}^{1/2}$ for 1 SE(B) specimens (see table 4). This is consistent with the 15% range of statistical variability of fracture toughness [33]. Hence, the

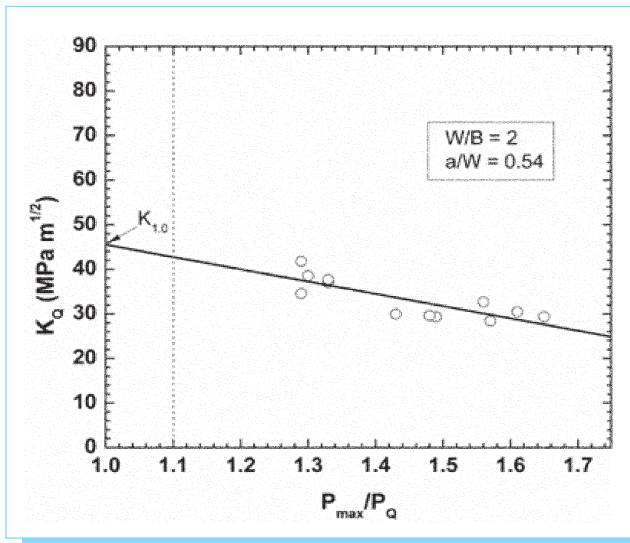


Fig. 11. $K_Q - P_{max}/P_Q$ relationship for data of 1Cr-1/2Ni cast steel. Stright line - data fitting with linear function.

value $K_{IC} = K_Q = 39.4 \text{ MPam}^{1/2}$ can be considered as a conservative estimate of the plane strain fracture toughness. This value is also consistent with data for other low-alloy cast steels reported in [29].

3.2. Size effect correlation

As it was mentioned above, the size effect on the apparent toughness K_Q is actively discussed in the literature. Some empirical relations were proposed to fit the correlations between K_Q and the specimen size parameters such as the thickness B , width W and ligament size $W - a$ [34-36]. In our experiments, the relations between these parameters were fixed as $W/B = 2$ and $0.54 < a/W < 0.55$ and so, there is no matter which of them is used to characterize the specimen size. Though, the ligament size seems to be a more appropriate parameter for this purpose [24,29]. Accordingly, we found that the best fit of our experimental data was provided by the following linear relationship

$$\frac{K_Q}{K_{IC}} = b \left[\frac{(W-a)_Q}{(W-a)_C} \right]^{1/2} + c \quad (5)$$

where b and c are fitting parameters, while $(W-a)_C$ is the critical ligament size (see Fig. 12). Furthermore, we found that the data for titanium alloy Ti-6Al-4V [35] and aluminum alloy 2219-T851 [36] obtained on specimens of the same geometrical relation ($W/B = 2$ and $a/W = 0.55$) also obey the

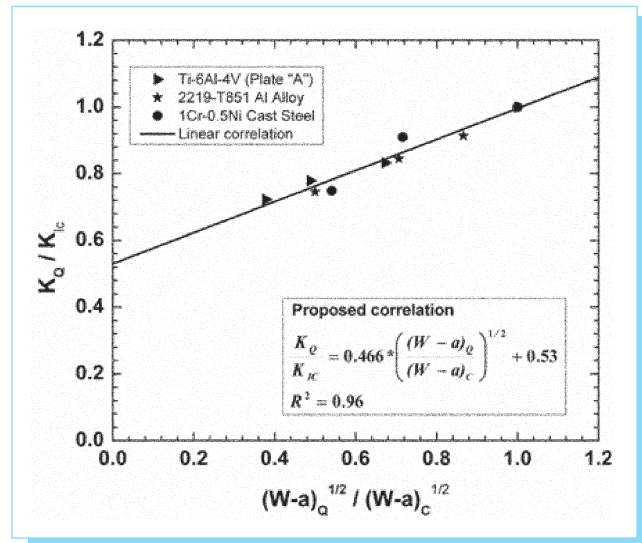


Fig. 12. Correlation between normalized apparent toughness K_Q/K_{IC} and the normalized ligament size for three different materials. All specimens with a ratio $W/B = 2$.

relation Eq. (5) with the same fitting parameters (see Fig. 12). This suggests that the fitting parameters b and c are independent of the material properties, but can be functions of geometric constrains W/B and a/W . Hence, Eq. (5) can be used for a fast estimate of plane strain fracture toughness K_{IC} from data obtained on sub-size specimens (see Table 4 and Fig. 13). Furthermore, the functional dependence of b and c on geometric constrains can be established in experiments with one or more metallic materials.

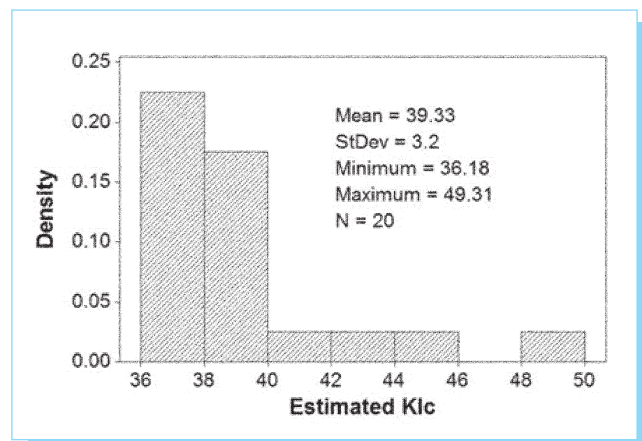


Fig. 13. Histogram of K_{IC} values obtained using Eq. (5).

4. Conclusions

1. The plane fracture toughness of 1Cr-½Ni cast steel was determined using subsize specimens. Although none of the specimens fully satisfied the fracture toughness criteria required by ASTM E399 standard, it was concluded that K_{Ic} value obtained for specimens satisfying the size requirement defined by Eq. (3), can be considered as the plane strain fracture toughness $K_{Ic} = 39.4 \pm 6 \text{ MPam}^{1/2}$, because criterion defined by Eq. (2) can be overlooked. It is mainly related to the steepness of tearing resistance curve, but not with the plane-strain measure.
2. The methodology employed in this work can be used in future studies, when there are restrictions of available material for the specimens required.
3. The empirical relationship (5) between the apparent toughness and ligament size is suggested. It can be used for a fast estimate of the plane strain toughness from the data obtained with subsize specimens.

Acknowledgments

The authors would like to thank Dr. Jorge Luis González Velázquez and Abel Hernández (ESIQIE-IPN) for the use of the scanning electron microscope facilities.

References

- [1] R. W. Hertzberg. *Deformation and Fracture Mechanics of Engineering Materials*. 3rd ed., New York: Wiley, 1989.
- [2] T. L. Anderson. *Fracture mechanics: fundamentals and applications*. 3rd ed., New York: CRC Press, 2005.
- [3] ASTM Designation E 399-09: *Standard Test Method for Linear-Elastic Plane-Strain Fracture Toughness K_{Ic} of Metallic Materials*. PA, USA: West Conshohocken, 2009.
- [4] R. Sarkar, & K. K. Ray, "Estimation of fracture toughness using miniature chevron-notched specimens". *Fatigue Fract. Eng. Mat. Struct.* 31, pp. 340-345, 2008.
- [5] W. J. Plumbridge, "New avenues for failure analysis". *Eng. Fail. Anal* 16, pp.1347-1354, 2009.
- [6] I. I. Cuesta, C. Rodríguez, F. J. Belzunce, & J. M. Alegre, "Analysis of different techniques for obtaining pre-cracked/notched small punch test specimens". *Eng. Fail. Anal*, 18, pp. 2282-2287, 2011.
- [7] S. F. Hoysan, & G. B. Sinclair, "On the variability of fracture toughness". *Int. J. Fract.* 1993, 60, pp. R43-R49.
- [8] G. B. Sinclair, M. Kondo, & R. V. Pieri, "The size dependence of fracture toughness for two embrittled materials". *Int. J. Fract.*, 72, pp. R3-R10, 1995.
- [9] A. S. Balankin, "The effect of fracture surface morphology on the crack mechanics in a brittle material". *Int. J. Fract.*, 76, pp. R63-R70, 1996.
- [10] A. S. Balankin, A. Bravo-Ortega, M. A. Galicia-Cortés, & O. Susarrey, "The effect of self-affine roughness on crack mechanics in elastic solids". *Int. J. Fract.*, 79, pp. R63-R68, 1996.
- [11] Z. X. Wang, H. J. Shi, & J. Lu, "Size effects on the ductile/brittle fracture properties of the pressure vessel steel 20 g". *Theor. Appl. Fract. Mech.*, 50, pp. 124-131, 2008.
- [12] A. S. Balankin, O. Susarrey, C. A. Mora, J. Patiño, A. Yoguez, & E. I. García, "Stress concentration and size effect in fracture of notched heterogeneous material". *Phys Rev, Ser. E*, 83, pp. 015101(R), 2011.
- [13] *Statistical Models for the Fracture of Disordered Media*. Eds. H. J. Herrmann & S. Roux, New York: Elsevier, 1990.
- [14] G. Palasantzas, "Roughness effects on the critical fracture toughness of materials under uniaxial stress". *J. Appl. Phys.*, 83, pp. 5212-5216, 1998.
- [15] G. P. Cherepanov, A. S. Balankin, & V. S. Ivanova, "Fractal Fracture Mechanics - a review". *Eng Fract Mech*, 51, pp. 997-1033, 1995.
- [16] A. S. Balankin, "Physics of fracture and mechanics of self-affine cracks". *Eng. Fract. Mech.*, 57, pp. 135-203, 1997.
- [17] A. S. Balankin, L. H. Hernández, G. Urriolagoitia, O. Susarrey, J. González, & J. Martínez, "Probabilistic mechanics of self-affine cracks in paper sheets". *Proc. R. Soc. Lond. A*, 455, pp. 2565-2575, 1999.
- [18] A. Yavari, S. Sarkani, E. T. Moyer, "The mechanics of self-similar and self-affine fractal cracks". *Int. J. Fract.*, 114, pp. 1-27, 2002.
- [19] Z. P. Bazant, & A. Yavari, "Is the cause of size effect on structural strength fractal or energetic-statistical?". *Eng. Fract. Mech.*, 72, pp. 1-31, 2005.
- [20] A. Carpinteri. "Scaling laws and renormalization groups for strength and toughness of disordered materials". *Int. J. Solids Struct.*, 31, pp. 291-302, 1994.
- [21] A. Carpinteri, & M. Corrado, "An extended (fractal) overlapping crack model to describe crushing size-scale effects in compression". *Eng. Fail. Anal*, 16, pp. 2530-2540, 2009.
- [22] M. J. Alava, P. K. V. V. Nukala, & S. Zapperi, "Size effects in statistical fracture". *J. Phys. D. Appl. Phys.*, 42, pp. 214012, 2009.
- [23] M. El-Shennawya, F. Minami, & M. Toyoda, K. Kajimoto, "Crack-tip plastic constraint activators and the application to plane-strain fracture toughness test: Proposal on small-size fracture toughness specimen". *Eng. Fract. Mech.*, 63, pp. 447-479, 1999.
- [24] K. R. W. Wallin, "Critical assessment of the standard ASTM E399". *J. ASTM Int.*, 2, pp. 433-453, 2005.
- [25] E. Wakai, H. Ohtsuka, S. Matsukawa, K. Furuya, H. Tanigawa, K. Okac, S. Ohnuki, T. Yamamoto, F.

- Takada, & S. Jitsukawa, "Mechanical properties of small size specimens of F82H steel". *Fusion Eng. Design*, 81, pp. 1077-1084, 2006.
- [26] J. Terán, J. L. González, J. M. Hallen, M. Martínez, "Efecto del tamaño de probeta y orientación en la resistencia a la tracción y a la tenacidad a la fractura". *Revista de Metalurgia*, 43, pp. 165-181, 2007.
- [27] M. Scibetta, J. Schuurmans, E. Lucon, & E. van Walle, "On the use of the crack tip opening angle parameter to explain the ductile crack growth behavior of miniature compact specimens". *Eng Fract Mech* 2008, 75, pp. 3599-3610.
- [28] K. Guan, L. Hua, Q. Wang, X. Zou, & M. Song, "Assessment of toughness in long term service CrMo low alloy steel by fracture toughness and small punch test". *Nuclear Eng. Design*, 241, pp. 1407-1413, 2011.
- [29] K. Wallin, "The size effect in K_{IC} ". *Eng. Fract. Mech.*, 1, pp. 149-163, 1985.
- [30] L. Santarelli, "A two-parameter method for determining the fracture toughness of materials from subsized specimens". *J. Test Eval. Am. Soc. Test Mat.*, 34, pp. 280-299, 2006.
- [31] ASTM Designation E 8M-04: Standard Test Method for Tension Testing of Metallic Materials. USA: West Conshohocken, 2004.
- [32] ASTM Designation E561-05: Standard Test Method for K-R Curve Determination. West Conshohocken, USA, 2005.
- [33] N. E. Dowling, *Mechanical behavior of materials, appendix B statistical variation in material properties*. 2nd ed., Prentice Hall, pp. 798-818, 1999.
- [34] S. Banerjee, "Influence of specimen size and configuration on the plastic zone size, toughness and crack growth". *Eng Fract Mech*, 1981, 15, pp. 343-390.
- [35] D. Munz, K. H. Galda, & F. Link, "Effect of specimen size on fracture toughness of a titanium alloy". *Mech. Crack Growth*, ASTM STP, 590, pp. 219-234, 1976.
- [36] J. G. Kaufman, & F. G. Nelson, *More on specimen size effects in fracture toughness testing*, ASTM STP 1974, 559, pp. 74-85.

Portal de portales Latindex

acceso a los contenidos y textos completos
de revistas académicas disponibles
en hemerotecas digitales de
América Latina, el Caribe,
España y Portugal

<http://www.latindex.ppl.unam.mx/>